InterTech presents

Synthetic Biology works

A Montagud
E Navarro
P Fernández de Córdoba
JF Urchueguía

- Toggle switch
- Repressilator
- Counting machine
  - ETH iGEM 2005
- Memory device
  - ETH iGEM 2007
- Cell free system
  - Imperial iGEM 2007
- Synthetic pattern formation
- Artificial Quorum Sensing
- Artemisinin production

Toggle switch

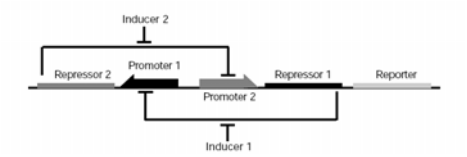

Toggle switch

NATURE | VOL 403 | 20 JANUARY 2000 | www.nature.com

Construction of a genetic toggle switch in *Escherichia coli*

Timothy S. Gardner*†, Charles R. Cantor* & James J. Collins*†

** Department of Biomedical Engineering, † Center for BioDynamics and ‡ Center for Advanced Biotechnology, Boston University, 44 Cummington Street, Boston, Massachusetts 02215, USA*

demonstrated in networks of non-specialized regulatory components. Here we present the construction of a genetic toggle switch—a synthetic, bistable gene-regulatory network—in *Escherichia coli* and provide a simple theory that predicts the conditions necessary for bistability. The toggle is constructed from any two repressible promoters arranged in a mutually inhibitory network. It is flipped between stable states using transient chemical or thermal induction and exhibits a nearly ideal switching threshold. As a practical device, the toggle switch forms a synthetic, addressable cellular memory unit and has implications for biotechnology, biocomputing and gene therapy.

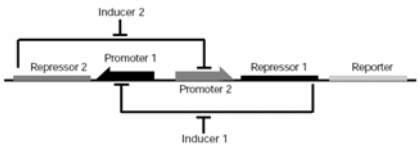

Figure 1 Toggle switch design. Repressor 1 inhibits transcription from Promoter 1 and is induced by Inducer 1. Repressor 2 inhibits transcription from Promoter 2 and is induced by Inducer 2.

Toggle switch

Box 1
The toggle model

The behaviour of the toggle switch and the conditions for bistability can be understood using the following dimensionless model for the network:

$$\frac{du}{dt} = \frac{\alpha_1}{1+v^{\beta}} - u \quad (1a)$$

$$\frac{dv}{dt} = \frac{\alpha_2}{1+u^{\gamma}} - v \quad (1b)$$

where u is the concentration of repressor 1, v is the concentration of repressor 2, α_1 is the effective rate of synthesis of repressor 1, α_2 is the effective rate of synthesis of repressor 2, β is the cooperativity of repression of promoter 2 and γ is the cooperativity of repression of promoter 1. The above model is derived from a biochemical rate equation formulation of gene expression[24–27]. The final form of the toggle equations preserves the two most fundamental aspects of the network: cooperative repression of constitutively transcribed promoters (the first term in each equation), and degradation/dilution of the repressors (the second term in each equation).

Figure 2

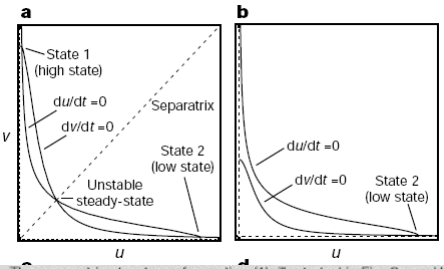

The geometric structure of equation (1), illustrated in Fig. 2a and b, reveals the origin of the bistability: the nullclines ($du/dt = 0$ and $dv/dt = 0$ in Fig. 2) intersect at three points, producing one unstable and two stable steady states. From Fig. 2a and b, three key features of the system become apparent. First, the nullclines intersect three times because of their sigmoidal shape, which arises for $\beta, \gamma > 1$. Thus, the bistability of the system depends on the cooperative repression of transcription. Second, the rates of synthesis of the two repressors must be balanced. If the rates are not balanced, the nullclines will intersect only once, producing a single stable steady state. This situation arises in plasmid pIKE105. Third, the structure of the toggle network creates two basins of attraction. Thus, a toggle with an initial condition anywhere above the separatrix will ultimately settle to state 1, whereas a toggle starting below the separatrix will settle to state 2.

Toggle switch

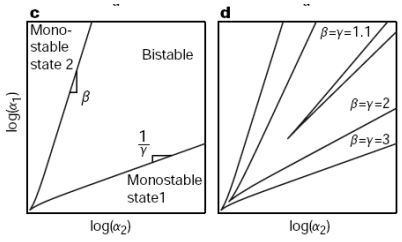

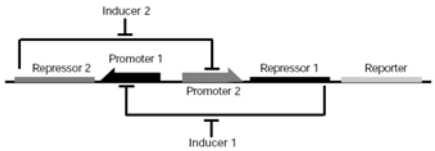

Figure 1 Toggle switch design. Repressor 1 inhibits transcription from Promoter 1 and is induced by Inducer 1. Repressor 2 inhibits transcription from Promoter 2 and is induced by Inducer 2.

The bistability of the toggle arises from the mutually inhibitory arrangement of the repressor genes. In the absence of inducers, two stable states are possible: one in which promoter 1 transcribes repressor 2, and one in which promoter 2 transcribes repressor 1. Switching is accomplished by transiently introducing an inducer of the currently active repressor. The inducer permits the opposing repressor to be maximally transcribed until it stably represses the originally active promoter.

Figure 2 Geometric structure of the toggle equations. **a**, A bistable toggle network with balanced promoter strengths. **b**, A monostable toggle network with imbalanced promoter strengths. **c**, The bistable region. The lines mark the transition (bifurcation) between bistability and monostability. The slopes of the bifurcation lines are determined by the exponents β and γ for large α_1 and α_2. **d**, Reducing the cooperativity of repression (β and γ) reduces the size of the bistable region. Bifurcation lines are illustrated for three different values of β and γ. The bistable region lies inside of each pair of curves.

Toggle switch

Figure 4 Demonstration of bistability.

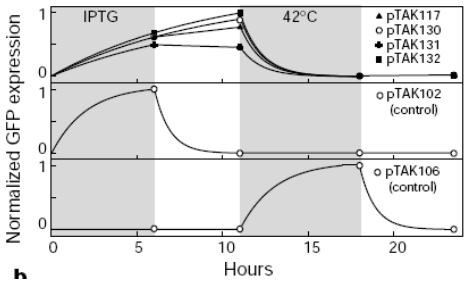

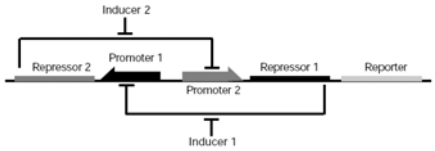

Figure 1 Toggle switch design. Repressor 1 inhibits transcription from Promoter 1 and is induced by Inducer 1. Repressor 2 inhibits transcription from Promoter 2 and is induced by Inducer 2.

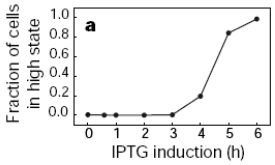

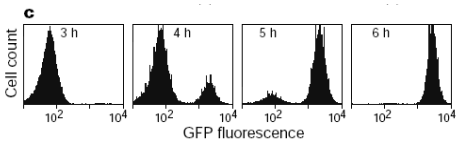

Figure 6 pTAK117 switching time.

Toggle switch

Figure 4 Demonstration of bistability.

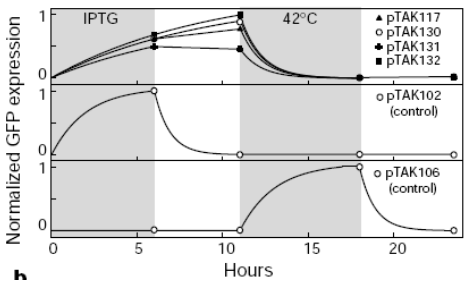

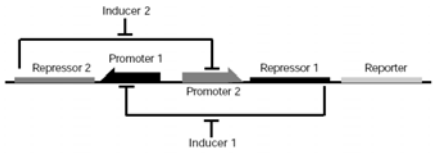

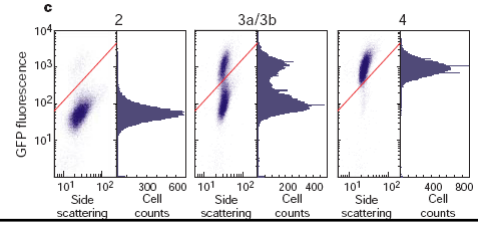

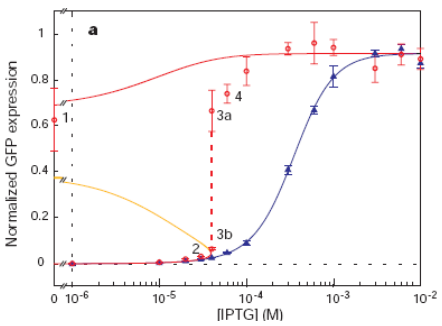

Figure 5

- pTAK117 — steady states
- pTAK102 — unsteady state

Table 1: Plasmids

Plasmid	Type	P1	RBS1	RBS2	GFP Expression
Bare Promoters					
pMKN7a*	I	Ptrc-2	E	—	732 ± 108
pBAG102	I	$P_L$tetO-1	C	—	5.5 ± 0.1
pBAG103	I	$P_L$tetO-1	A	—	660 ± 42
pBRT21.1*	I	P_Ls1con	D	—	9,390 ± 840
pBRT21.1*†	I	P_Ls1con	D	—	14,300 ± 400
pBRT123	I	P_Ls1con	G	—	387 ± 21
pBRT124	I	P_Ls1con	F	—	972 ± 43
pBRT125	I	P_Ls1con	H	—	15.9 ± 3.2
lacI Repression					
pTAK102	II	P_Ls1con	D	—	36.0 ± 3.8
pTAK103a	II	P_Ls1con	G	—	137 ± 8
cI Repression					
pTAK106	III	P_Ls1con	D	—	2.5 ± 0.3
pTAK107	III	P_Ls1con	G	—	2.0 ± 0.1
tetR Repression					
pIKE108	III	$P_L$tetO-1	A	—	5.8 ± 1.0
pIKE110	III	$P_L$tetO-1	C	—	2.3 ± 0.2
Toggles					
pTAK117	IV	P_Ls1con	D	B	bistable
pTAK130	IV	P_Ls1con	G	B	bistable
pTAK131	IV	P_Ls1con	F	B	bistable
pTAK132	IV	P_Ls1con	H	B	bistable
pIKE105	IV	$P_L$tetO-1	A	B	monostable
pIKE107	IV	$P_L$tetO-1	C	B	bistable

*Estimated from flow-cytometer assay of GFPuv-expressing promoters.
†Grown at 32°C.

Repressilator

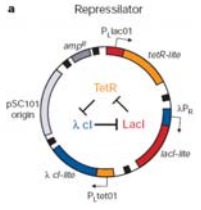

Repressilator

NATURE | VOL 403 | 20 JANUARY 2000 | www.nature.com

A synthetic oscillatory network of transcriptional regulators

Michael B. Elowitz & Stanislas Leibler

Departments of Molecular Biology and Physics, Princeton University, Princeton, New Jersey 08544, USA

synthetic network to implement a particular function. We used three transcriptional repressor systems that are not part of any natural biological clock[3–5] to build an oscillating network, termed the repressilator, in *Escherichia coli*. The network periodically induces the synthesis of green fluorescent protein as a readout of its state in individual cells. The resulting oscillations, with typical periods of hours, are slower than the cell-division cycle, so the state of the oscillator has to be transmitted from generation to generation. This artificial clock displays noisy behaviour, possibly because of stochastic fluctuations of its components. Such 'rational network design' may lead both to the engineering of new cellular behaviours and to an improved understanding of naturally occurring networks.

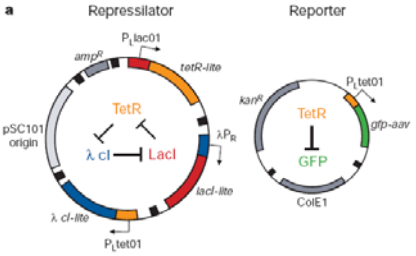

Repressilator

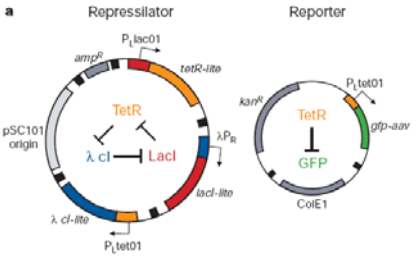

Figure 1

Deterministic, continuous approximation

Three repressor-protein concentrations, p_i, and their corresponding mRNA concentrations, m_i (where i is *lacI*, *tetR* or *cI*) were treated as continuous dynamical variables. Each of these six molecular species participates in transcription, translation and degradation reactions. Here we consider only the symmetrical case in which all three repressors are identical except for their DNA-binding specificities. The kinetics of the system are determined by six coupled first-order differential equations:

$$\frac{dm_i}{dt} = -m_i + \frac{\alpha}{(1+p_j^n)} + \alpha_0 \qquad \begin{pmatrix} i = lacI, tetR, cI \\ j = cI, lacI, tetR \end{pmatrix}$$

$$\frac{dp_i}{dt} = -\beta(p_i - m_i)$$

where the number of protein copies per cell produced from a given promoter type during continuous growth is α_0 in the presence of saturating amounts of repressor (owing to the 'leakiness' of the promoter), and $\alpha + \alpha_0$ in its absence; β denotes the ratio of the protein decay rate to the mRNA decay rate; and n is a Hill coefficient. Time is rescaled in units of the mRNA lifetime; protein concentrations are written in units of K_M, the number of repressors necessary to half-maximally repress a promoter; and mRNA concentrations are rescaled by their translation efficiency, the average number of proteins produced per mRNA molecule. The numerical solution of the model shown in Fig. 1c used the following parameter values: promoter strength, 5×10^{-4} (repressed) to 0.5 (fully induced) transcripts per s; average translation efficiency, 20 proteins per transcript, Hill coefficient, $n = 2$; protein half-life, 10 min; mRNA half-life, 2 min; K_M, 40 monomers per cell.

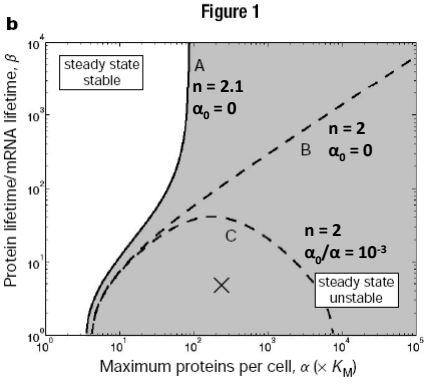

Repressilator

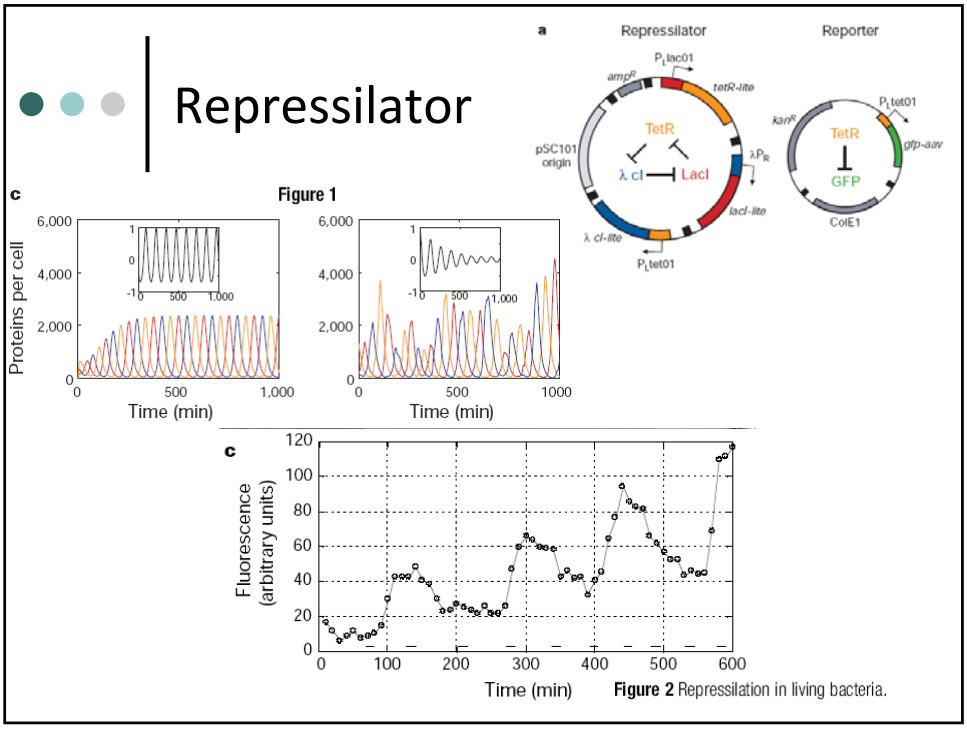

Repressilator

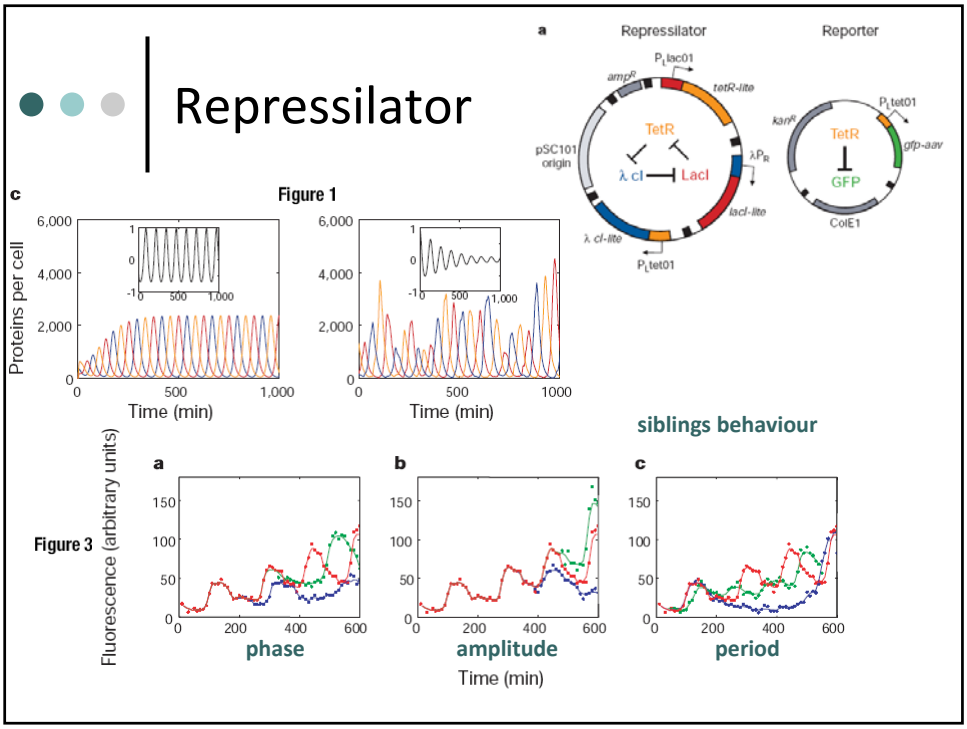

Counting machine

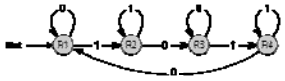

ETHZ iGEM 2005

Counting machine

ETHZ iGEM 2005

http://parts.mit.edu/wiki/index.php/ETH_Zurich_2005

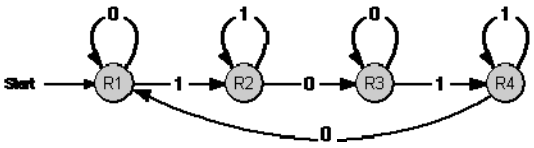

The counter is a finite state machine implemented as a genetic circuit. It has 4 internal states *R1* to *R4*. The **transition between these states is induced by an external stimulus** with values 0 and 1 - denoting whether it is absent or present, respectively. Repeated stimulus will lead to successive transitions and finally to repeated cycling through those 4 states.

Each time the state R4 is reached, an output signal is generated. This leads to a counting behavior where every second occurence of 1 (high signal) is indicated by the output signal.

Counting machine

ETHZ iGEM 2005

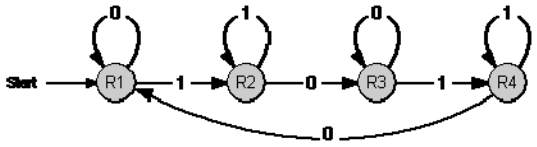

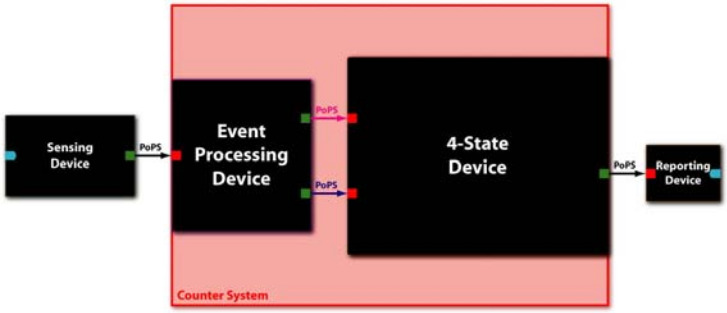

Counting machine

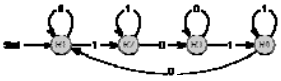

ETHZ iGEM 2005

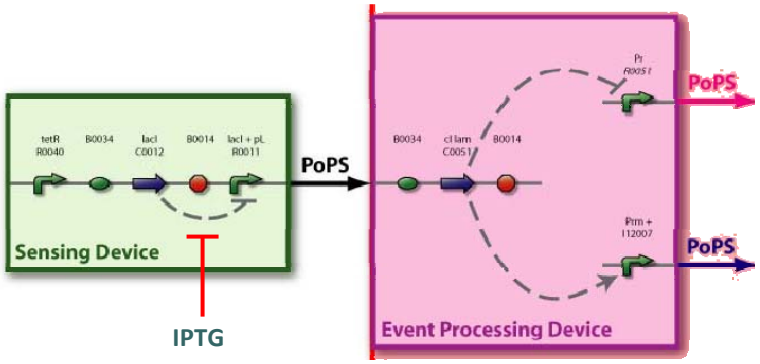

Counting machine

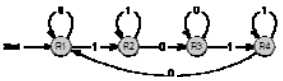

ETHZ iGEM 2005

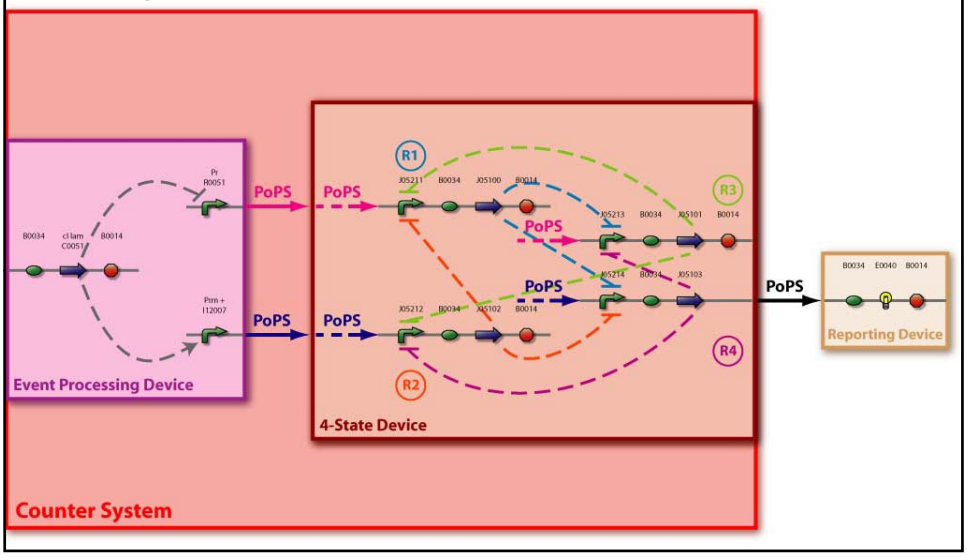

Counting machine

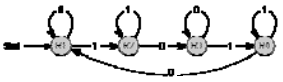

ETHZ iGEM 2005

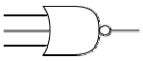

NOR gate

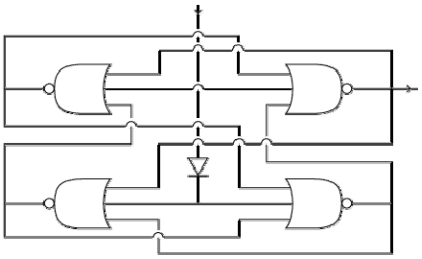

Biologically, a NOR gate can be implemented through a promoter with **high basal activity that is repressed by three effectors**. If there is at least one of the three repressors, transcription is inhibited.

Counting machine

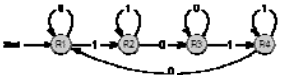

ETHZ iGEM 2005

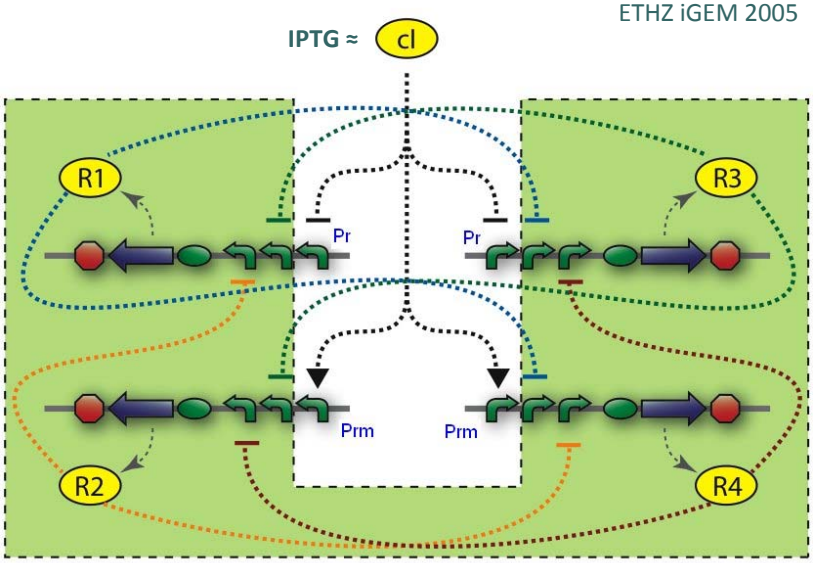

Counting machine

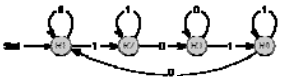

ETHZ iGEM 2005

dR1/dt = k_syn_R1 · rep(S) · rep(R2) · rep(R3) - k_deg_R1 · R1

dR2/dt = k_syn_R2 · act(S) · rep(R3) · rep(R4) - k_deg_R2 · R2

dR3/dt = k_syn_R3 · rep(S) · rep(R1) · rep(R4) - k_deg_R3 · R3

dR4/dt = k_syn_R4 · act(S) · rep(R1) · rep(R2) - k_deg_R4 · R4

$$act(A) = \frac{\left(\frac{A}{K_{act}}\right)^n}{1+\left(\frac{A}{K_{act}}\right)^n} \qquad rep(R) = \frac{1}{1+\left(\frac{R}{K_{rep}}\right)^n}$$

Counting machine

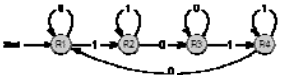

ETHZ iGEM 2005

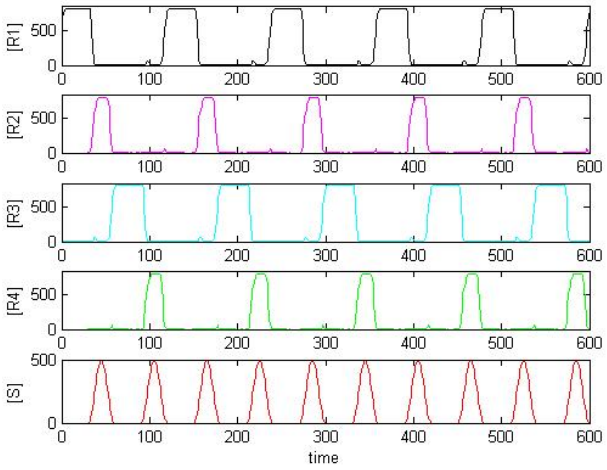

Memory device

*educat*ETH

ETHZ iGEM 2007

Memory device

*educat*ETH

http://parts.mit.edu/igem07/index.php/ETHZ

ETHZ iGEM 2007

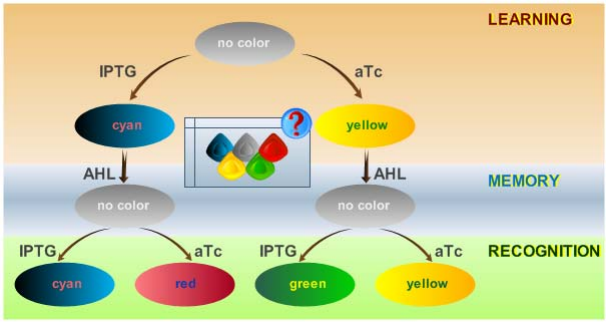

Fig. 1: Flow diagram. This figure shows the protocol with which the final system should be tested as well as the test results in form of the reported colors. The protocol is divided into three phases: (1) a training or learning phase in which the system learns an input and stores it in its memory, (2) a memory phase in which the system keeps the content of its memory, and finally (3) a recognition phase where the output of the system depends on the content of its memory as well as the current input.

Memory device

*educat*ETH

ETHZ iGEM 2007

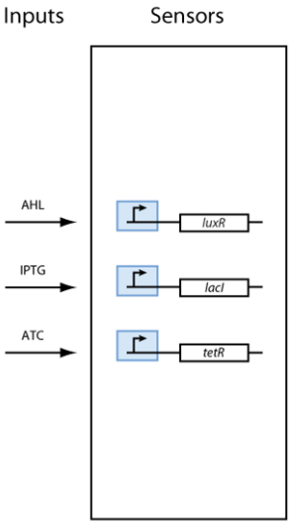

- two learning inputs
  - ATC
  - IPTG
- one memory input
  - AHL

Memory device

*educat*ETH

ETHZ iGEM 2007

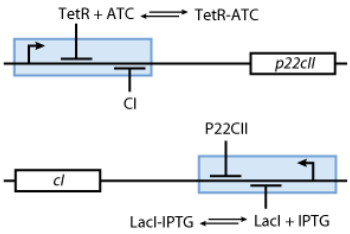

- t_0 : *learning*
  - CI & P22CII = 0
- ATC ⟶ P22CII
- IPTG ⟶ CI

Memory device

*educat*ETH

ETHZ iGEM 2007

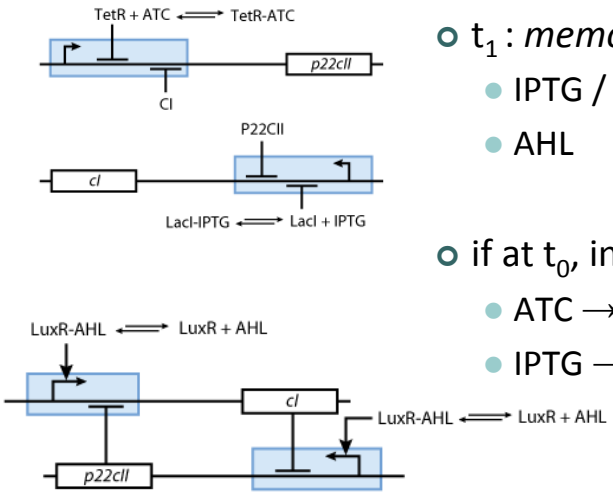

- t_1 : *memory*
  - IPTG / ATC removed
  - AHL
- if at t_0, in cell :
  - ATC ⟶ P22CII ctes
  - IPTG ⟶ CI ctes

Memory device

*educat*ETH

ETHZ iGEM 2007

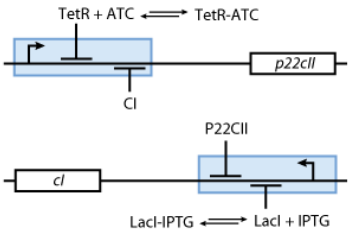

- t_2 : *recognition*
  - ATC
  - IPTG
- if at t_0, in cell :
  - ATC → P22CII
  - IPTG → CI

Memory device

*educat*ETH

ETHZ iGEM 2007

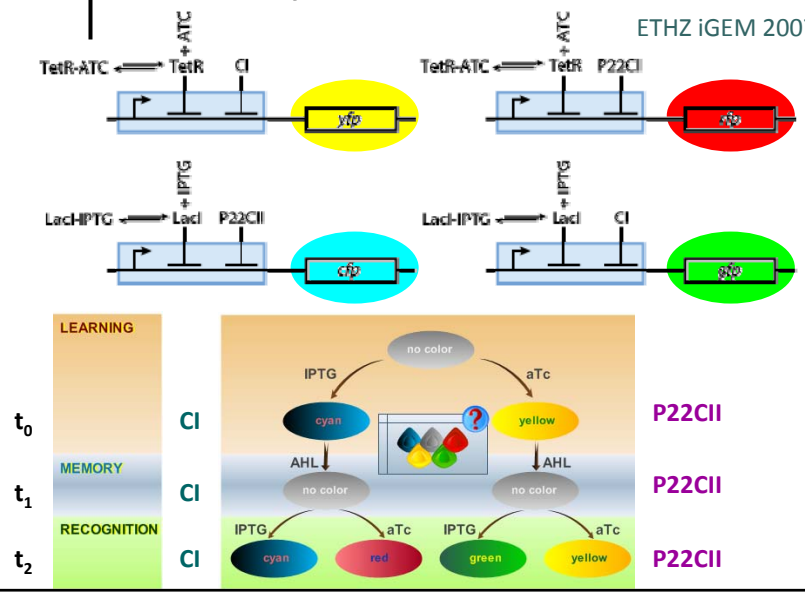

t_0 CI P22CII

t_1 CI P22CII

t_2 CI P22CII

Cell-free system

Cell-free system

http://parts.mit.edu/igem07/index.php/Imperial

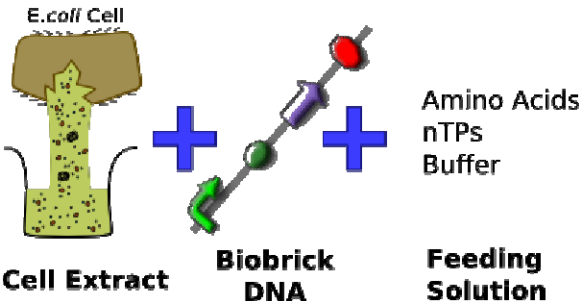

eukaryote or prokaryote

transcription or transcription + translation

Cell-free system

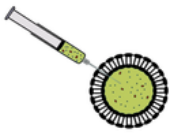

- Batch-mode CFS
  - transcription-translation in bulk solution
  - expression limited by nutrients & energy
- Continuous-exchange CFS
  - transcription-translation in dialysis membrane
  - expression sustained by diffusion of nutrients
  - wastes diluted in feeding solution
- Vesicule encapsulated CFS
  - phospholipid bilayer separates from solution
  - maintained for a longer time period because of membrane diffusion
  - non-specific pore protein increases reliability of material exchange

Cell-free system

Advantages	Disadvantages
System is not restricted by the policies imposed on genetically modified organisms	**Short expression lifespan** because of limited energy of the system even in the presence of an ATP regenerating system
Process is quick and simple requiring only preparation of cell extract and feeding solution and subsequent addition of DNA template	**Expensive system** has no sustained metabolism to convert cheap energy (like sugars) into useable one for the gene expression machinery
No concurrent expression of existing genome, therefore your genetically engineered device is **more energy efficient**	Less characterization and experience of use in the laboratories compared to *E. coli*
No DNA mutation of your genetically engineered device because there is no DNA replication	
No selective pressure on your genetically engineered device because the system is non-living and does not undergo natural selection	
No self-replication of your genetically engineered device leads to a **fixed amount of DNA being expressed** and **more control over the rate of expression**	
Expression system can be quality-controlled by manipulating adjustable parameters e.g. buffers are added to maintain optimum magnesium concentrations for efficient translation; protease inhibitors can be added to minimize degradation of synthesized proteins	

Cell-free system

Imperial College London iGEM 2007

homemade *E. coli* CFS

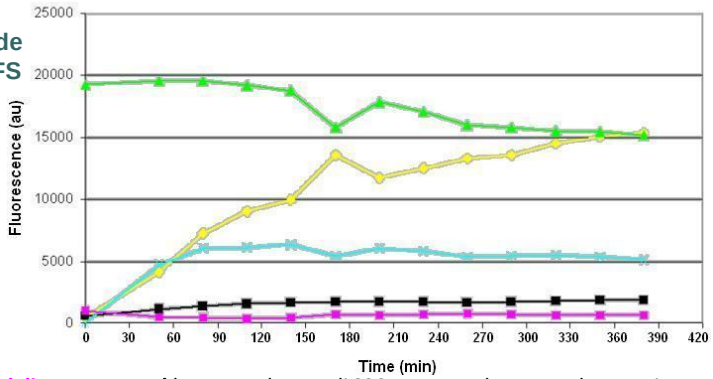

pink line : **– control** homemade *E. coli* S30 extract + homemade premix no DNA
blue line : homemade *E. coli* S30 extract + homemade premix + DNA
yellow line : commercial *E. coli* S30 extract + commercial premix + DNA
black line : homemade *E. coli* S30 extract + commercial premix + DNA
green line : **+ control** GFP protein in solution

Cell-free system

Imperial College London iGEM 2007

commercial *E. coli* CFS

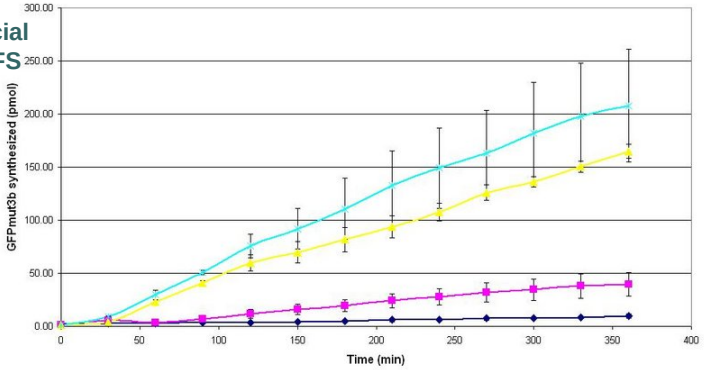

dark blue line : 8ºC
pink line : 15ºC
yellow line : 20ºC
blue line : 30ºC

Synthetic pattern formation

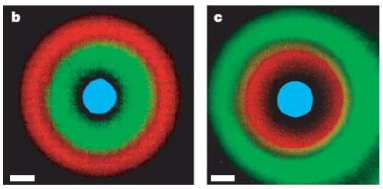

Synthetic pattern formation

A synthetic multicellular system for programmed pattern formation

Subhayu Basu[1], Yoram Gerchman[1], Cynthia H. Collins[3], Frances H. Arnold[3] & Ron Weiss[1,2]

[1]*Department of Electrical Engineering and* [2]*Department of Molecular Biology, Princeton University, Princeton, New Jersey 08544, USA*
[3]*Division of Chemistry and Chemical Engineering, California Institute of Technology 210-41, Pasadena, California 91125, USA*

NATURE | VOL 434 | 28 APRIL 2005 | www.nature.com/nature

Pattern formation is a hallmark of coordinated cell behaviour in both single and multicellular organisms[1–3]. It typically involves cell–cell communication and intracellular signal processing. Here we show a synthetic multicellular system in which genetically engineered 'receiver' cells are programmed to form ring-like patterns of differentiation based on chemical gradients of an acyl-homoserine lactone (AHL) signal that is synthesized by 'sender' cells. In receiver cells, 'band-detect' gene networks respond to user-defined ranges of AHL concentrations. By fusing different fluorescent proteins as outputs of network variants, an initially undifferentiated 'lawn' of receivers is engineered to form a bullseye pattern around a sender colony. Other patterns, such as ellipses and clovers, are achieved by placing senders in different configurations. Experimental and theoretical analyses reveal which kinetic parameters most significantly affect ring development over time. Construction and study of such synthetic multicellular systems can improve our quantitative understanding of naturally occurring developmental processes and may foster applications in tissue engineering, biomaterial fabrication and biosensing.

Synthetic pattern formation

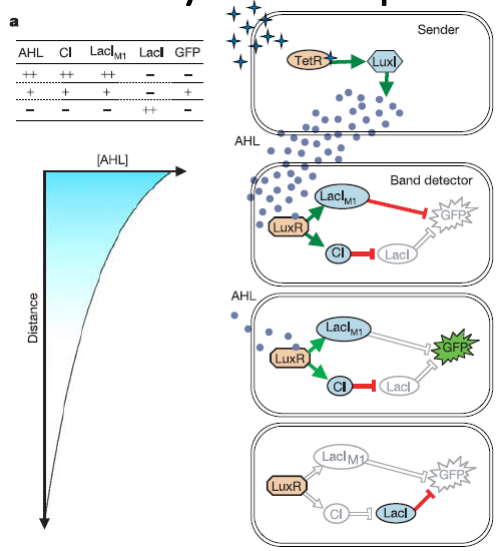

Figure 1 The band-detect multicellular system programs *E. coli* receiver cells to fluoresce only at intermediate distances from sender cells. **a**, Circuit operation for a sender and

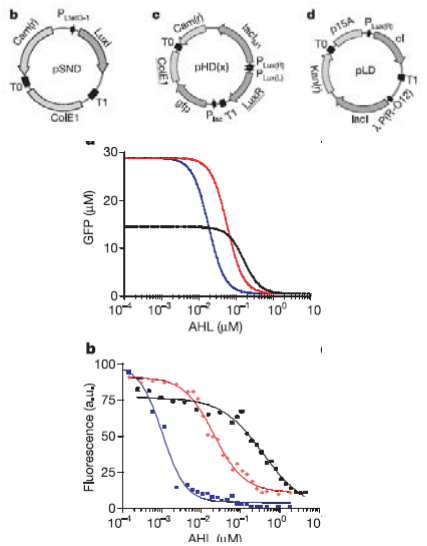

Figure 2 Simulated and experimental liquid-phase behaviour of high-detect and band-detect networks. **a**, **b**, Simulations (**a**) and experimental results (**b**) of the AHL dosage

Synthetic pattern formation

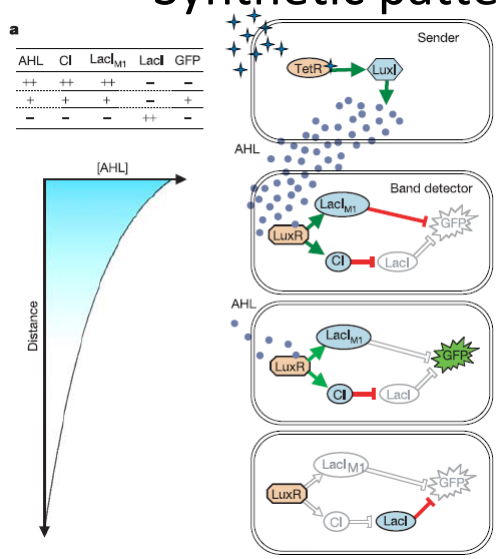

Figure 1 The band-detect multicellular system programs *E. coli* receiver cells to fluoresce only at intermediate distances from sender cells. **a**, Circuit operation for a sender and

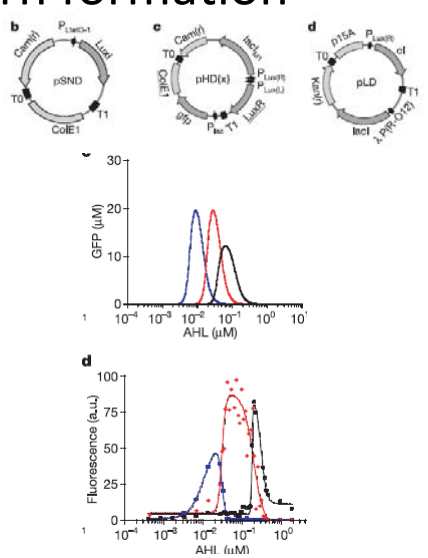

Figure 2 Simulated and experimental liquid-phase behaviour of high-detect and band-detect networks. **a**, **b**, Simulations (**a**) and experimental results (**b**) of the AHL dosage

Synthetic pattern formation

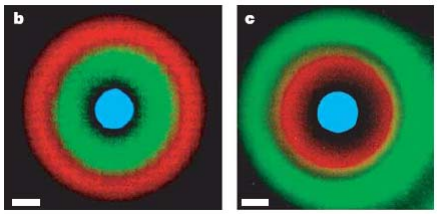

Figure 3 Experimental solid-phase behaviour of band-detect networks. a

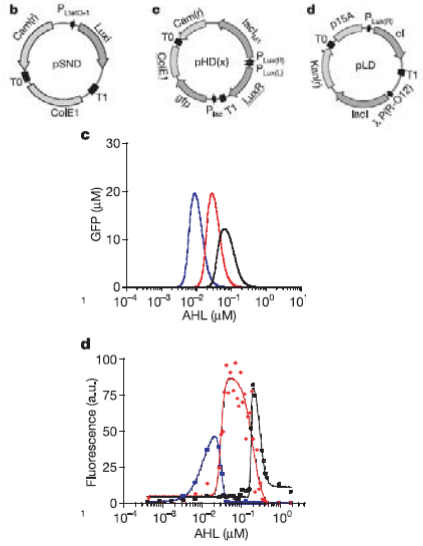

Figure 2 Simulat… of high-detect and band-detect networks. **a**, **b**, Simulations (**a**) and experimental results (**b**) of the AHL dosage

Synthetic pattern formation

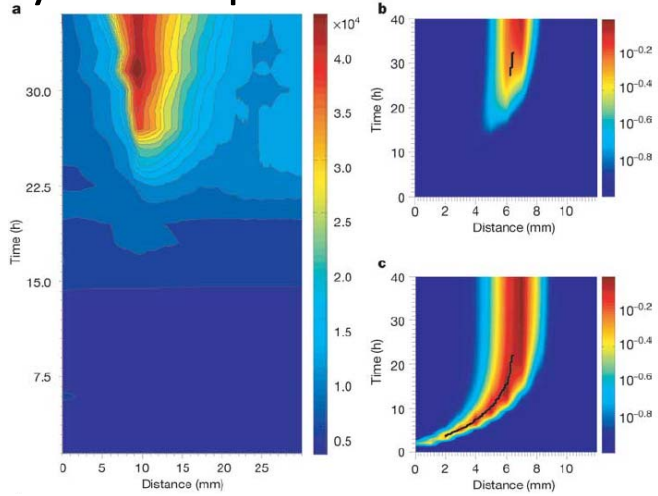

Figure 4 Ring formation dynamics. **a**, Experimental results showing the time-evolution of fluorescence for band-detect cells as a function of the distance from the senders. **b**, **c**, Spatiotemporal simulations of two shifts with different sets of kinetic parameters that form the ring at the same distance. Maximal levels of fluorescence are indicated by red, while the black lines represent the spatiotemporal shift of the ring. The shift associated with a fast decaying LacI (**c**) is larger than the shift resulting from a stable LacI (**b**). **d**, Regression analysis correlating the fluorescence response times with rate constants for LacI decay. Open triangles, shift end; filled diamonds, shift begin. **e**, Regression analysis correlating positional shift with rate constants for LacI decay.

Synthetic pattern formation

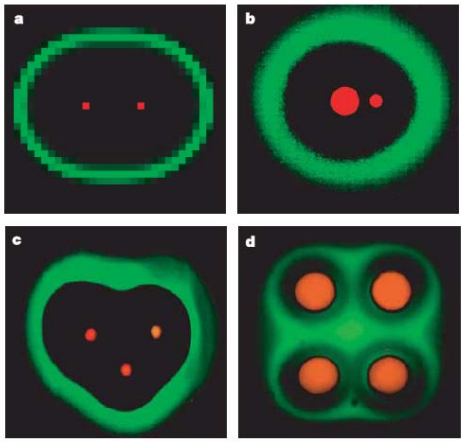

Figure 5 Formation of various patterns. **a**, Simulation of band-detect behaviour on solid media with two senders that results in the formation of an ellipse. **b–d**, Experimental results showing various GFP patterns formed based on the placement and initial concentrations of sender cells expressing DsRed-Express: **b**, ellipse, two sender disks; **c**, heart, three sender disks; and **d**, clover, four sender disks.

Artificial Quorum Sensing

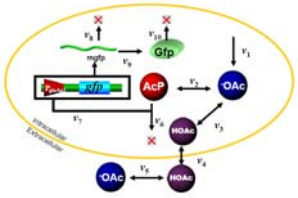

Artificial Quorum Sensing

PNAS | February 24, 2004 | vol. 101 | no. 8 | 2299–2304

Design of artificial cell–cell communication using gene and metabolic networks

Thomas Bulter*, Sun-Gu Lee*†, Wilson WaiChun Wong*, Eileen Fung‡, Michael R. Connor*, and James C. Liao*§

*Department of Chemical Engineering and ‡Biomedical Engineering Interdepartmental Program, University of California, Los Angeles, CA 90095

Artificial transcriptional networks have been used to achieve novel, nonnative behavior in bacteria. Typically, these artificial circuits are isolated from cellular metabolism and are designed to function without intercellular communication. To attain concerted biological behavior in a population, synchronization through intercellular communication is highly desirable. Here we demonstrate the design and construction of a gene-metabolic circuit that uses a common metabolite to achieve tunable artificial cell–cell communication. This circuit uses a threshold concentration of acetate to induce gene expression by acetate kinase and part of the nitrogen-regulation two-component system. As one application of the cell–cell communication circuit we created an artificial quorum sensor. Engineering of carbon metabolism in *Escherichia coli* made acetate secretion proportional to cell density and independent of oxygen availability. In these cells the circuit induced gene expression in response to a threshold cell density. This threshold can be tuned effectively by controlling ΔpH over the cell membrane, which determines the partition of acetate between medium and cells. Mutagenesis of the enhancer sequence of the $glnAp_2$ promoter produced variants of the circuit with changed sensitivity demonstrating tunability of the circuit by engineering of its components. The behavior of the circuit shows remarkable predictability based on a mathematical design model.

- Integrate
  - intercellular comunication : quorum sensing
  - cellular metabolism : acetate
  - transcriptional regulation : GFP
- Tunable circuit

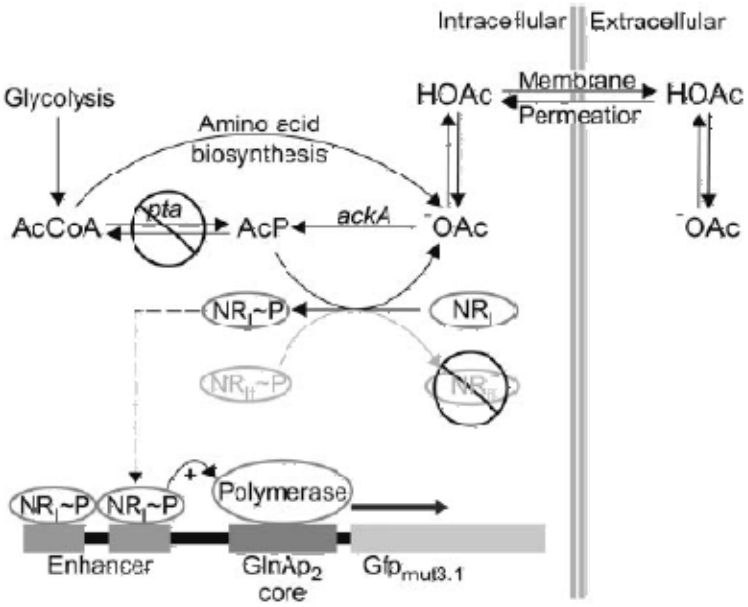

Artificial Quorum Sensing

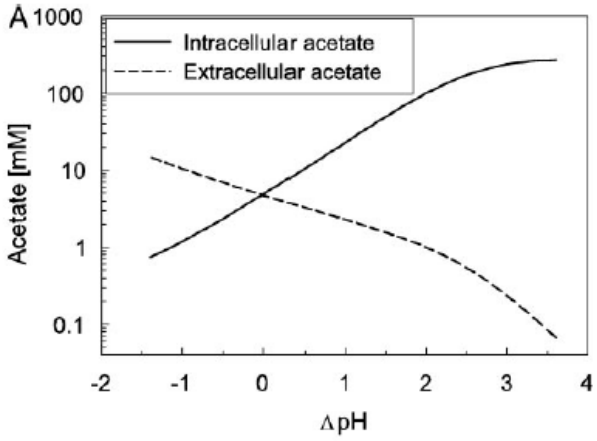

ΔpH =
pH(int) – pH(ext)

pH(int) = 7.6
pH(ext) = 5 - 8

Artificial Quorum Sensing

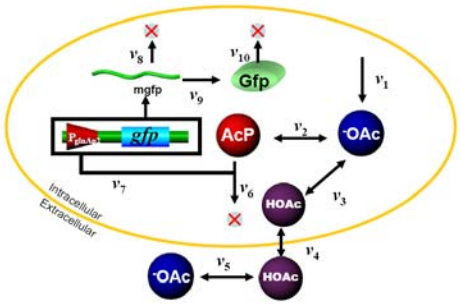

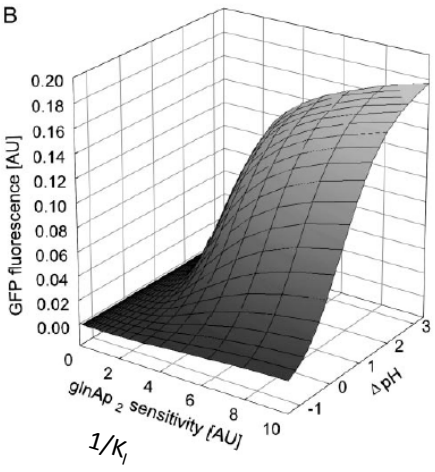

system after 10 hours

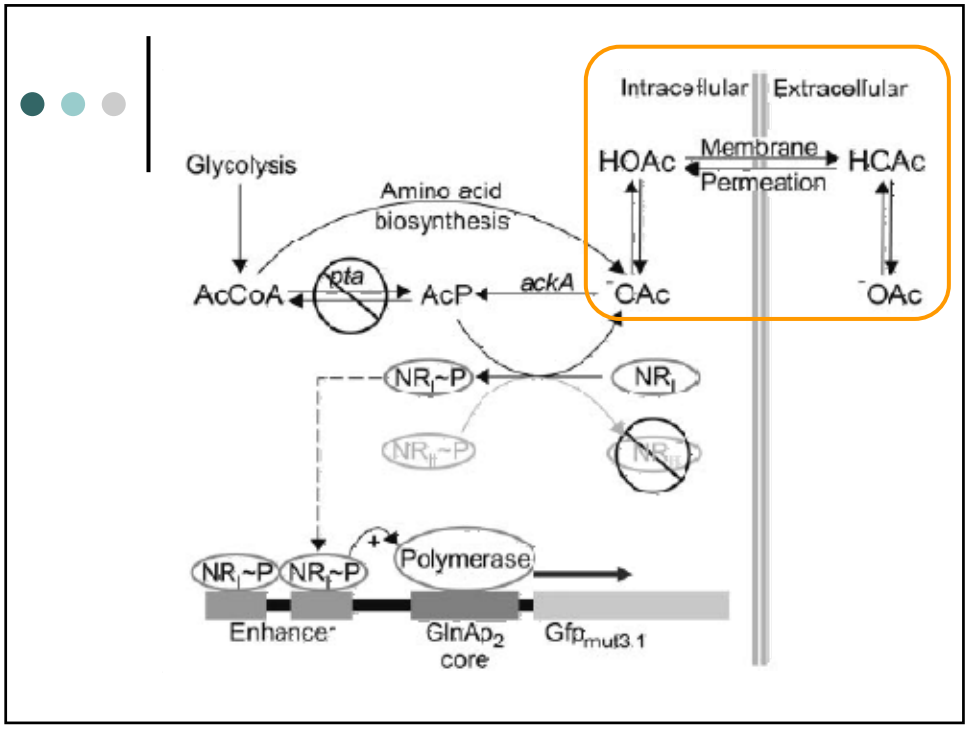

Artificial Quorum Sensing

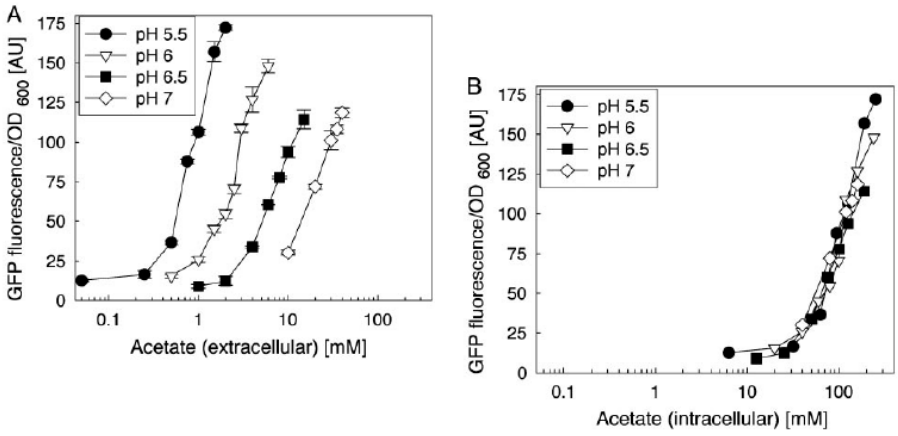

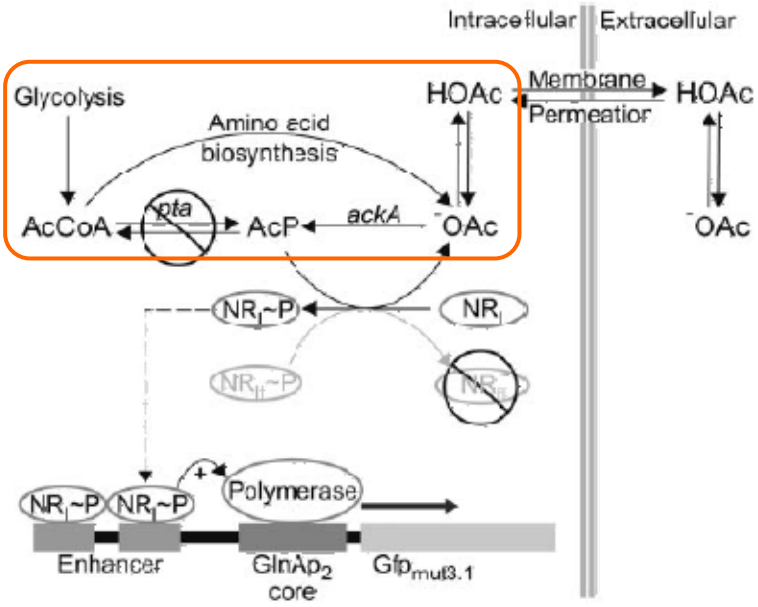

Artificial Quorum Sensing

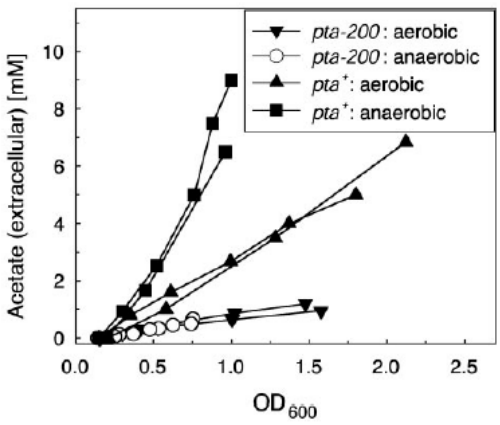

- in anaerobic conditions, *E. coli* produces more acetate
- without *pta*, extracel·lular [acetate] is not afected by oxygen condition

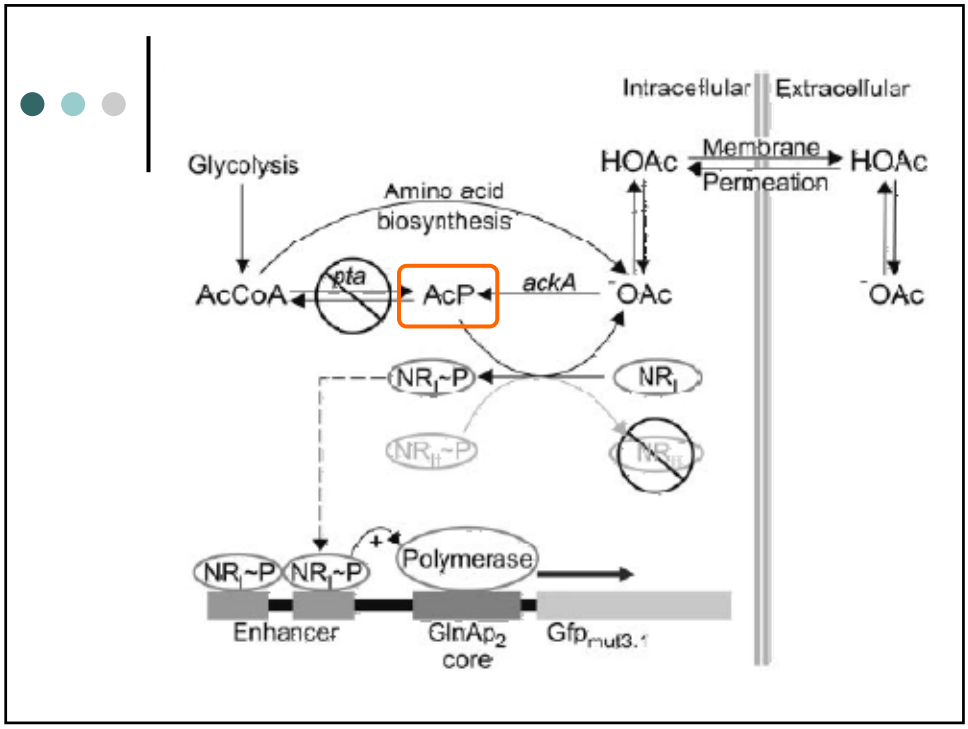
Intracellular
Extracellular
Glycolysis
HOAc
Membrane
Permeation
HOAc
Amino acid
biosynthesis
AcCoA
pta
AcP
ackA
OAc
OAc
NR$_I$~P
NR$_I$
NR$_{II}$~P
NR$_{II}$
NR$_I$~P
NR$_I$~P
Polymerase
Enhancer
GlnAp$_2$
core
Gfp$_{mut3.1}$

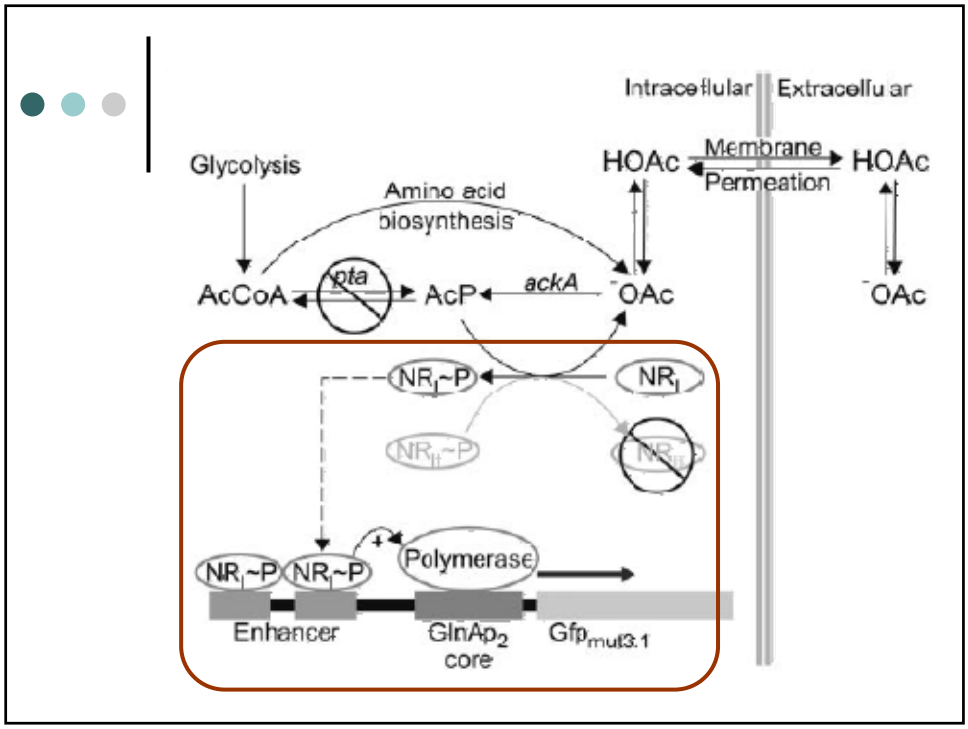
Intracellular
Extracellular
Glycolysis
HOAc
Membrane
Permeation
HOAc
Amino acid
biosynthesis
AcCoA
pta
AcP
ackA
OAc
OAc
NR$_I$~P
NR$_I$
NR$_{II}$~P
NR$_{II}$
NR$_I$~P
NR$_I$~P
Polymerase
Enhancer
GlnAp$_2$
core
Gfp$_{mut3.1}$

Artificial Quorum Sensing

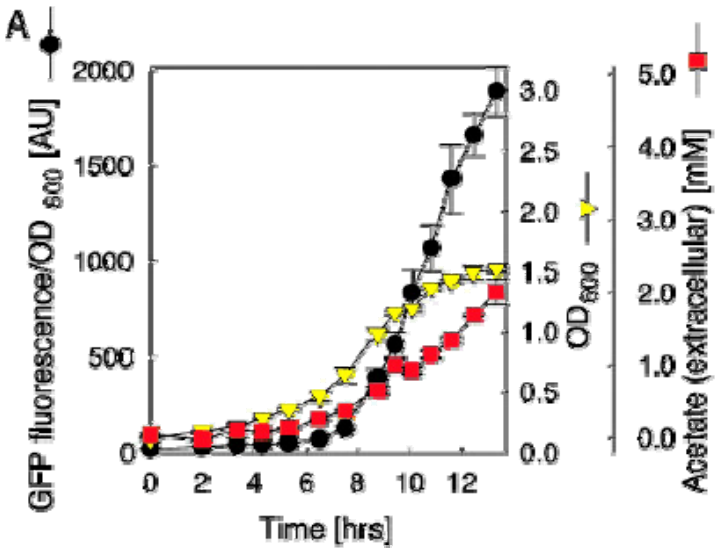

Artificial Quorum Sensing

tuning parameters

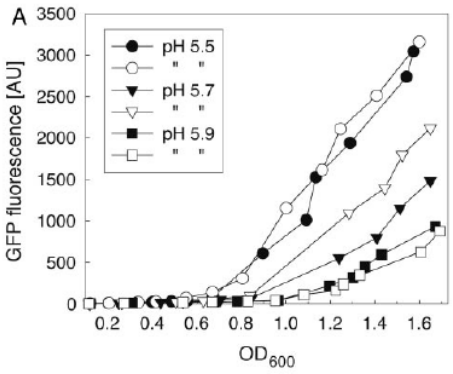

pH

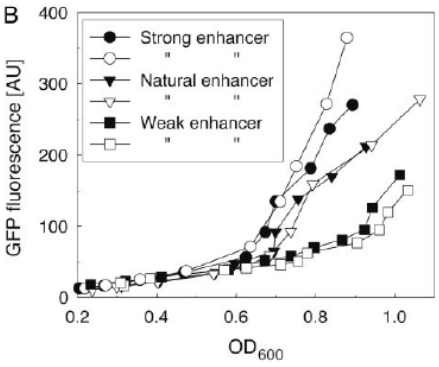

promoter

Artificial Quorum Sensing

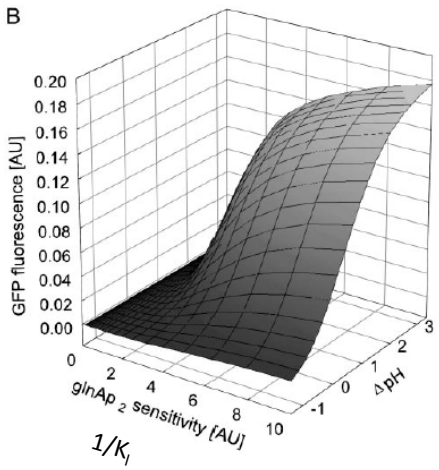

pH(int) – pH(ext)

system after 10 hours

Conclusions

- System works as a ‘quorum sensor’
  - acetate, signal molecule, produced constantly
  - signal diffuses membrane
  - [acetate] relates to cell density
  - GFP expression only when a threshold is reached
- Mathematical model predicts acurately the system’s behaviour

Artemisinin production

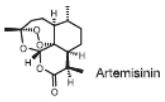

Artemisinin production

nature Vol 440|13 April 2006|doi:10.1038/nature04640

Production of the antimalarial drug precursor artemisinic acid in engineered yeast

Dae-Kyun Ro[1]*, Eric M. Paradise[2]*, Mario Ouellet[1], Karl J. Fisher[6], Karyn L. Newman[1], John M. Ndungu[3], Kimberly A. Ho[1], Rachel A. Eachus[1], Timothy S. Ham[4], James Kirby[2], Michelle C. Y. Chang[1], Sydnor T. Withers[2], Yoichiro Shiba[2], Richmond Sarpong[3] & Jay D. Keasling[1,2,4,5]

Malaria is a global health problem that threatens 300–500 million people and kills more than one million people annually[1]. Disease control is hampered by the occurrence of multi-drug-resistant strains of the malaria parasite *Plasmodium falciparum*[2,3]. Synthetic antimalarial drugs and malarial vaccines are currently being developed, but their efficacy against malaria awaits rigorous clinical testing[4,5]. Artemisinin, a sesquiterpene lactone endoperoxide extracted from *Artemisia annua* L (family Asteraceae; commonly known as sweet wormwood), is highly effective against multi-drug-resistant *Plasmodium* spp., but is in short supply and unaffordable to most malaria sufferers[6]. Although total synthesis of artemisinin is difficult and costly[7], the semi-synthesis of artemisinin or any derivative from microbially sourced artemisinic acid, its immediate precursor, could be a cost-effective, environmentally friendly, high-quality and reliable source of artemisinin[8,9]. Here we report the engineering of *Saccharomyces cerevisiae* to produce high titres (up to 100 mg l^{-1}) of artemisinic acid using an engineered mevalonate pathway, amorphadiene synthase, and a novel cytochrome P450 monooxygenase (*CYP71AV1*) from *A. annua* that performs a three-step oxidation of amorpha-4,11-diene to artemisinic acid. The synthesized artemisinic acid is transported out and retained on the outside of the engineered yeast, meaning that a simple and inexpensive purification process can be used to obtain the desired product. Although the engineered yeast is already capable of producing artemisinic acid at a significantly higher specific productivity than *A. annua*, yield optimization and industrial scale-up will be required to raise artemisinic acid production to a level high enough to reduce artemisinin combination therapies to significantly below their current prices.

Artemisinin production

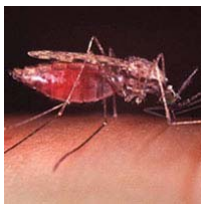

- *Anopheles* mosquito with *Plasmodium falciparum* parasite causes malaria
- Artemisinin from *Artemisina annua* is highly effective against multi-drug-resistant *Plasmodium*
  - short supply
  - expensive
- Total chemical synthesis is difficult and expensive

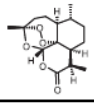

Goals

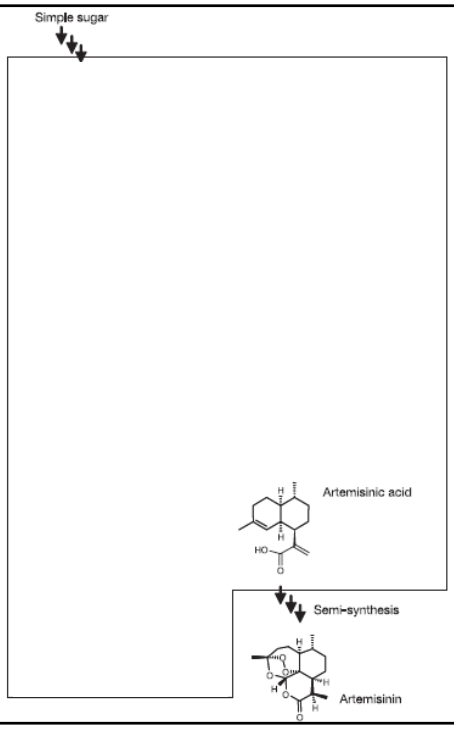

- *Saccharomyces cerevisae*
- semi-synthesis to artemisinic acid

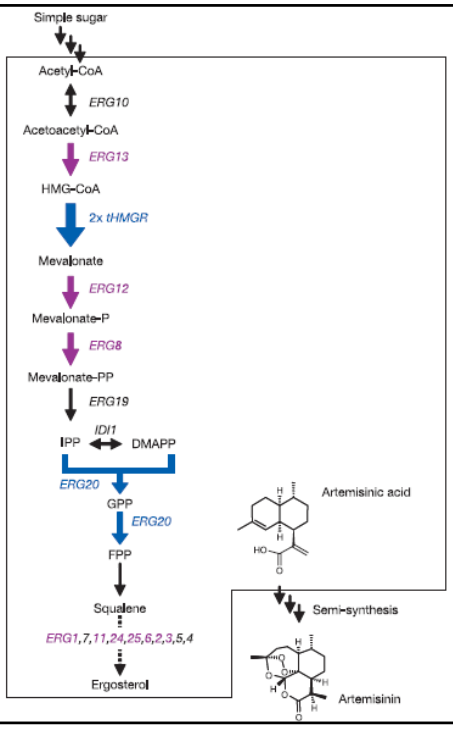

- *Saccharomyces cerevisae*
- semi-synthesis to artemisinic acid
- mevalonate pathway

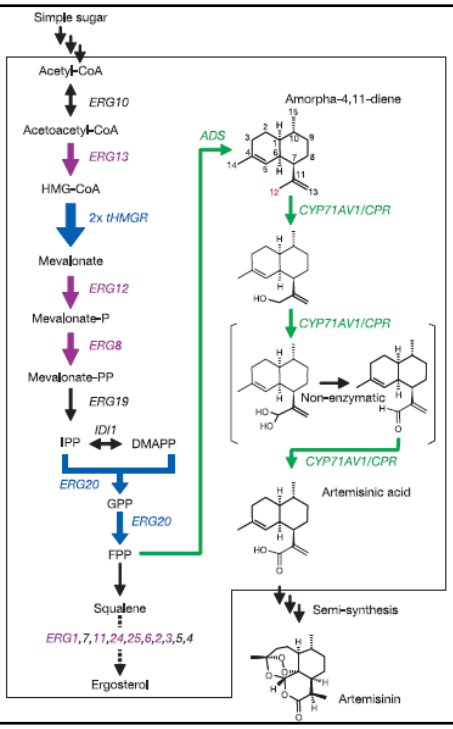

- *Saccharomyces cerevisae*
- semi-synthesis to artemisinic acid
- mevalonate pathway
- *A. annua*:
  - amorphadiene synthase
  - novel cytochrome P450 monooxygenase

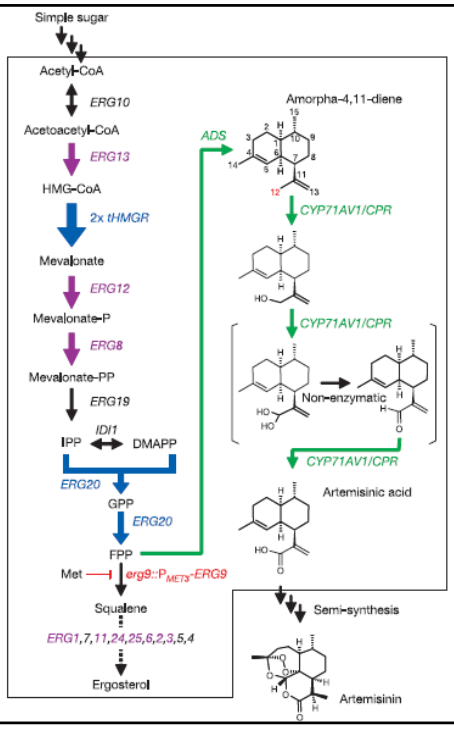

- *Saccharomyces cerevisae*
- semi-synthesis to artemisinic acid
- mevalonate pathway
- *A. annua*:
  - amorphadiene synthase
  - novel cytochrome P450 monooxygenase
- Overall metabolic tuning
  - overexpressions
  - inhibition

Artemisinin production

1. Adjusting the mevalonate pathway
2. From amorphadiene to artemisinic acid
3. Artemisinic acid analysis

1- Adjusting the mevalonate pathway

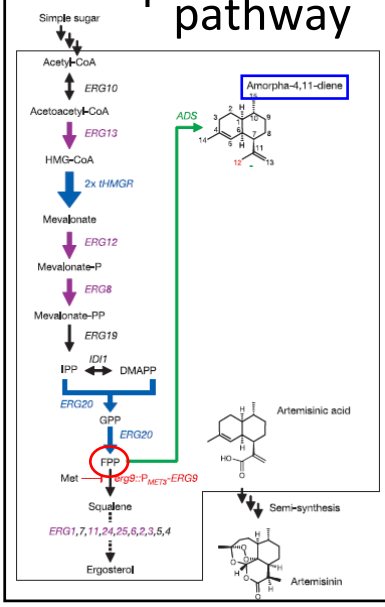

- increase farnesil pyrophosphate (FPP) production
- decrease sterols generation

- ADS from *A. annua*
- measuring [amorphadiene] by strains

[amorphadiene] by strains

- ADS with GAL1 promoter

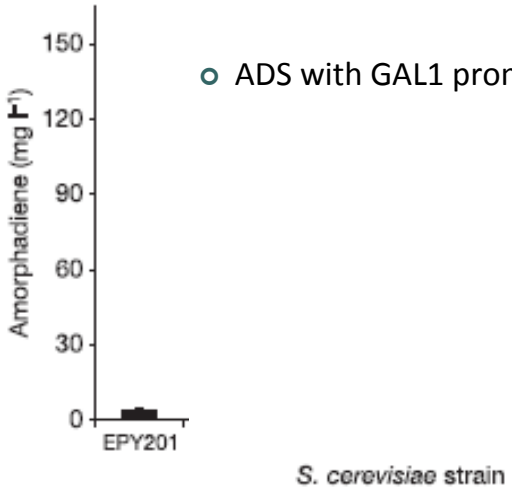

[amorphadiene] by strains

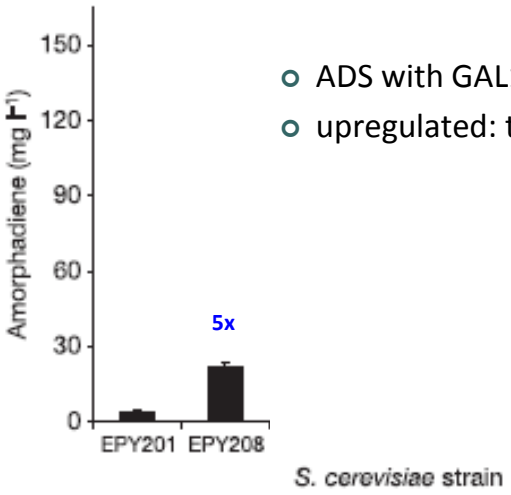

- ADS with GAL1 promoter
- upregulated: tHMGR

[amorphadiene] by strains

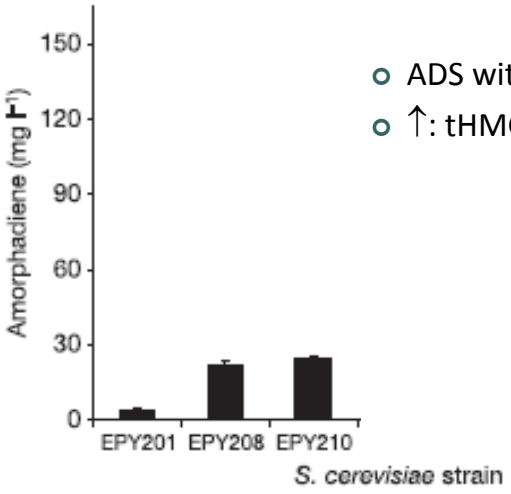

- ADS with GAL1 promoter
- ↑: tHMGR, upc2-1 (↓sterol TF)

[amorphadiene] by strains

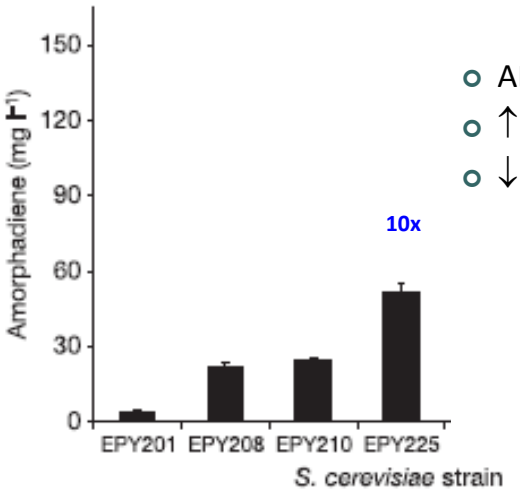

- ADS with GAL1 promoter
- ↑ : tHMGR
- ↓ : erg9

[amorphadiene] by strains

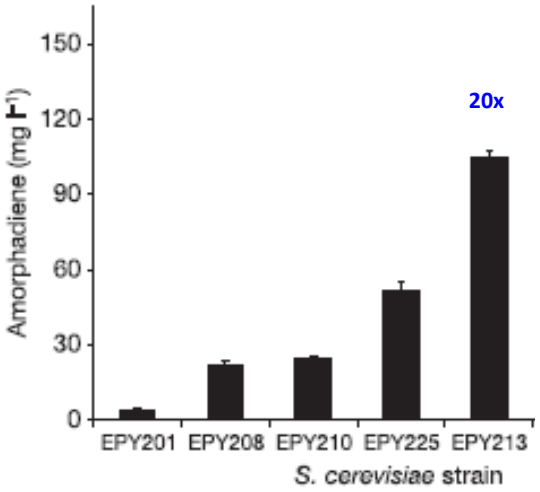

- ADS with GAL1 promoter
- ↑ : tHMGR, upc2-1
- ↓ : erg9

[amorphadiene] by strains

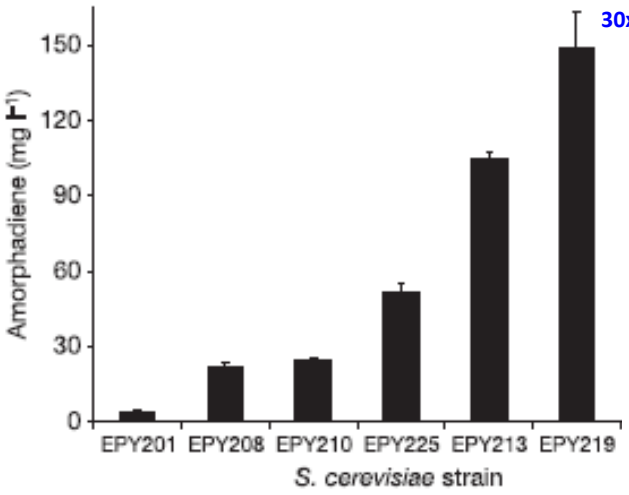

- ADS with GAL1 promoter
- ↑ : upc2-1
- ↓ : erg9
- 2 x tHMGR

[amorphadiene] by strains

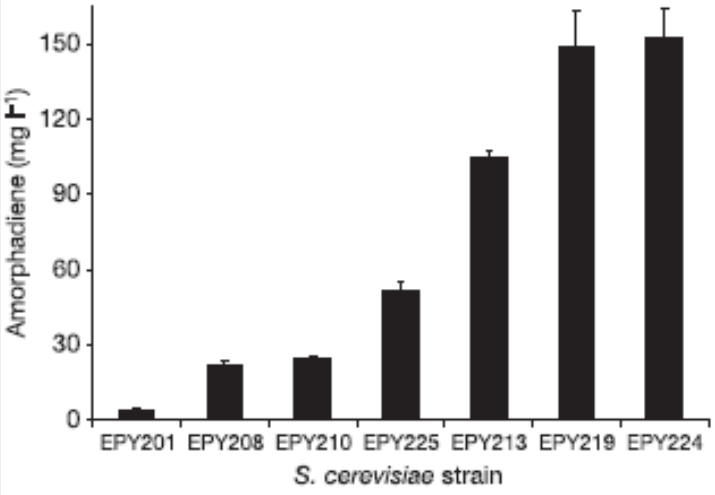

- pGAL1-ADS
- ↑ : upc2-1
- ↓ : erg9
- 2 x tHMGR
- ↑ : erg20

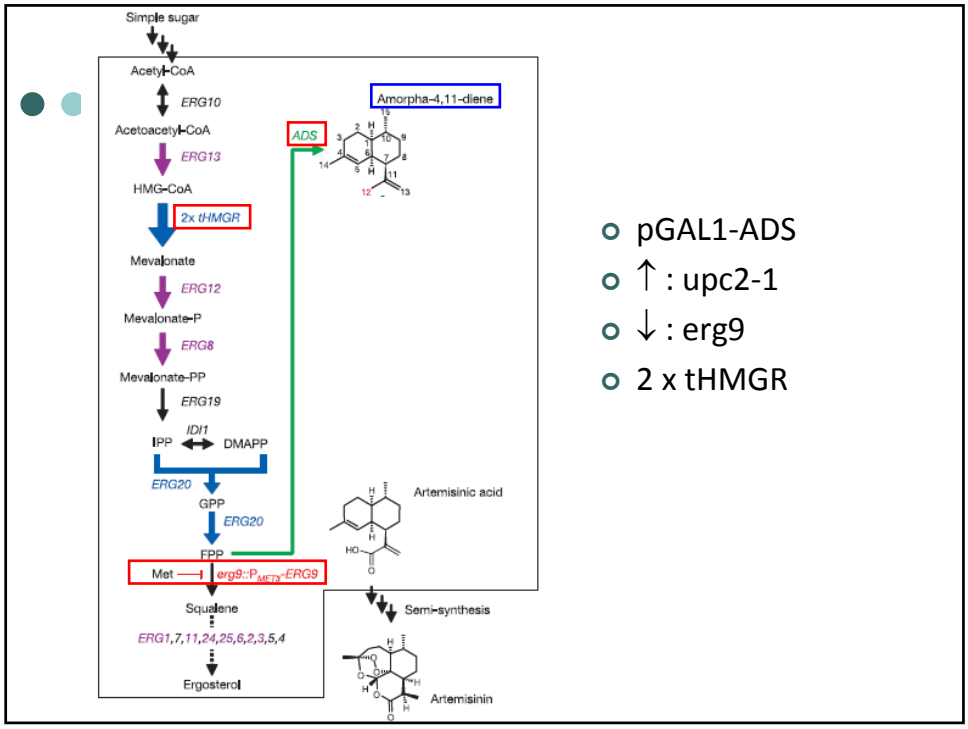

- pGAL1-ADS
- ↑ : upc2-1
- ↓ : erg9
- 2 x tHMGR

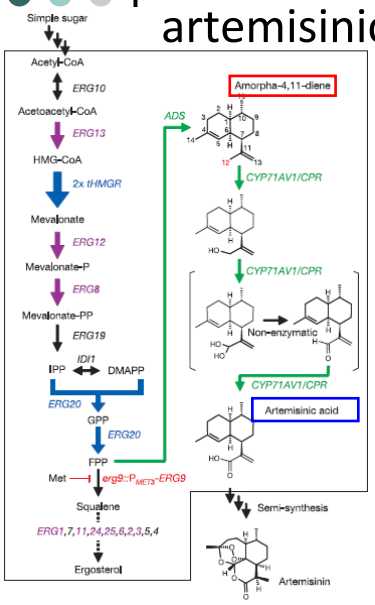

2- From amorphadiene to artemisinic acid

- what enzyme?
  - previous clues for a *A. annua* cytochrome P450
- which one? comparative genomics
  - Asteraceae family would share common ancestors enzymes for the early steps of the sesquiterpene lactones synthesis

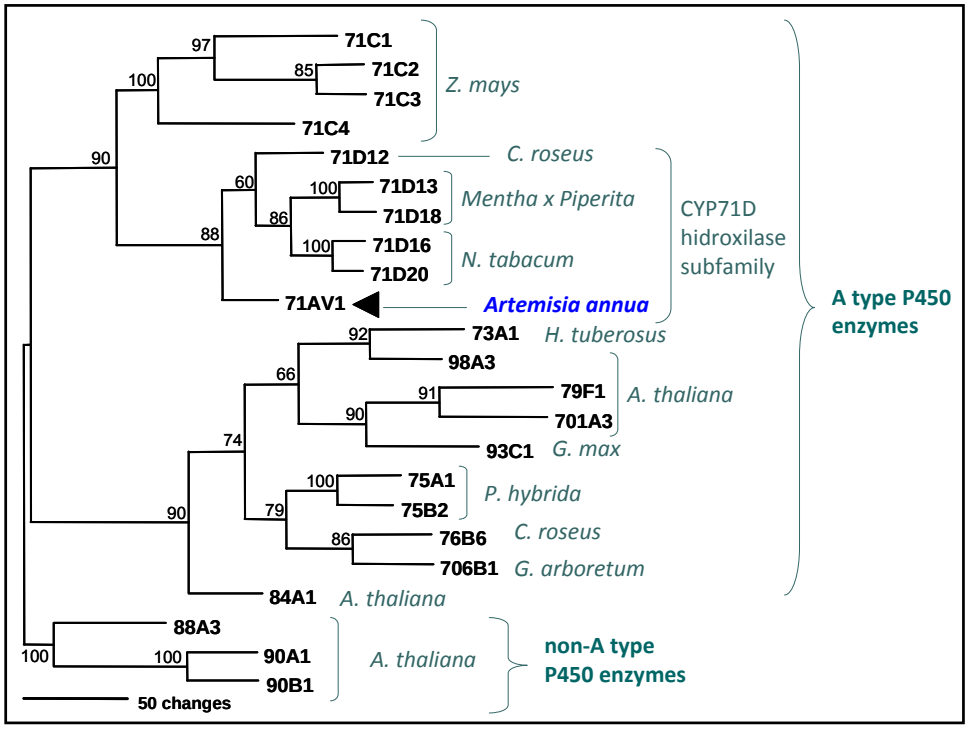

3- Artemisinic acid analysis

- isolation of:
  - CYP71AV1
  - CPR : native redox partner, NADPH:cytochrome P450 oxidoreductase
- EPY224 transformed with both genes
- culture medium analysed by gas chromatography mass spectrometry looking for artimisinic acid

GC-MS analysis

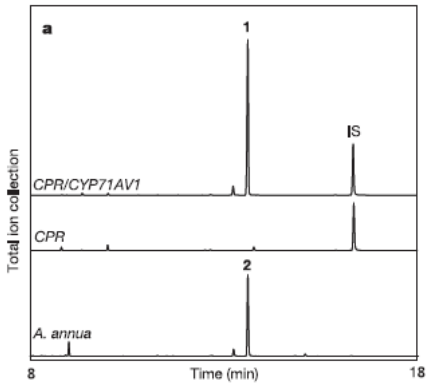

- transgenic yeast and A. annua share a peak → artemisinic acid
- negative control does not

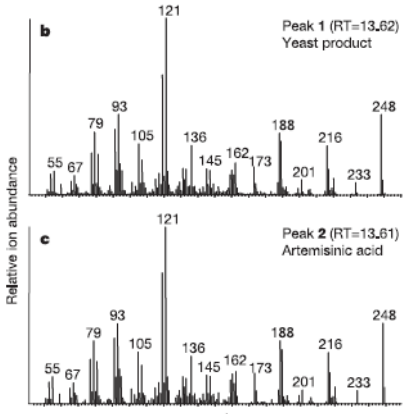

- transgenic yeast product correlates with artemisinic acid

artimisinin purification

- > 96 % of the synthetised artemisinic acid was removed from the cell pellet by washing with alkaline buffer
- therefore, artemisinic acid is transported out of the cell, but remains bound to cell surface on acidic medium

- a one-step purification method was developed:
  - 1) ether extraction of the culture medium
  - 2) silica gel column chromatographic separation

CYP71AV1 activities

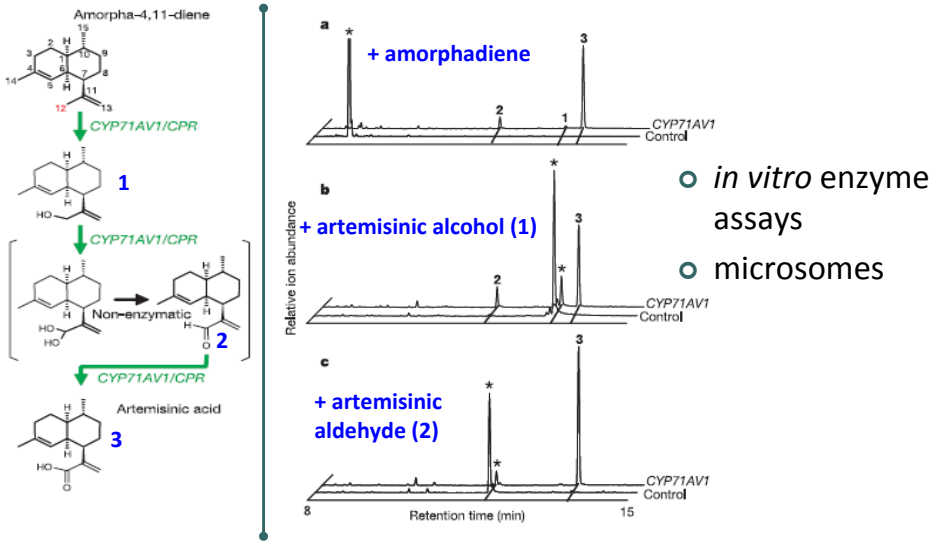

- *in vitro* enzyme assays
- microsomes

Scientifical conclusions

- Transgenic yeast effectively produces artemisinic acid
- Artemisinic acid is produced at a biomass fraction comparable to that produced by *A. annua* but over a much shorter time (4-5 days vs. several months)
- 100x specific productivity for yeast vs. *A. annua*

Medical conclusions

- Given the existence of known, relatively high yielding chemistry for the conversion of artemisinic acid to artemisinin microbially produced artemisinic acid is a viable source of this potent family of antimalarial drugs
- A conservative analysis suggests that artemisinin combination therapies could be offered significantly below their current prices
- In addition to cost savings, this bioprocess should not be subject to factors like weather or political climates that may affect plant cultivation

sources

InterTech

- Gardner *et al*, *Construction of a genetic toggle switch in* Escherichia coli. **Nature**. 2000
- Elowitz & Leibler, *A synthetic oscillatory network of transcriptional regulators*. **Nature**. 2000
- http://parts.mit.edu/wiki/index.php/ETH_Zurich_2005
- http://parts.mit.edu/igem07/index.php/ETHZ
- http://parts.mit.edu/igem07/index.php/Imperial
- Basu *et al*, *A synthetic multicellular system for programmed pattern formation*. **Nature**. 2005
- Bulter *et al, Design of artificial cell–cell communication using gene and metabolic networks.* **PNAS**. 2004
- Ro *et al, Production of the antimalarial drug precursor artemisinic acid in engineered yeast*. **Nature**. 2006